

## A Study of Aftershocks of the 17 July 1998 Ruey-Li, Chiayi Earthquake

Kou-Cheng Chen<sup>1</sup>, Bor-Shouh Huang<sup>1</sup>, Kuo-Liang Wen<sup>1</sup>, Hung-Chie Chiu<sup>1</sup>,  
Yeong-Tein Yeh<sup>1</sup>, Shih-Nan Cheng<sup>1</sup>, Han-Yih Peng<sup>1</sup>, Tao-Ming Chang<sup>1</sup>,  
Tzay-Chyn Shin<sup>2</sup>, Ruey-Chyuan Shih<sup>3</sup> and Ching-Ren Lin<sup>1,4</sup>

(Manuscript received 22 January 1999, in final form 7 July 1999)

### ABSTRACT

On 17 July 1998, an earthquake of magnitude 6.2 ( $M_L$ ) occurred near Chiayi, southwestern Taiwan. Two days after the occurrence of the mainshock, a temporary digital seismic network was deployed near its epicenter for 24 days to monitor the aftershock activity. The events within and near the network were first located using a traditional single-event location and then relocated using a joint hypocentral determination (JHD) technique to determine the significance of lateral velocity variations and to improve earthquake locations. The station corrections obtained from the JHD analysis vary from 0.30 to -0.18 sec for the P-waves and from 0.51 to -0.58 sec for the S-waves. The patterns of station corrections suggest that upper crustal velocities on the eastern side of the study area are relatively higher than those on the western side. The depth cross-section of the relocated aftershocks shows a clear pattern of southeast-dipping distribution of the hypocenters. The focal mechanisms and hypocentral distribution of the relocated aftershocks reveal a close relationship between seismicity and the known faults in the study area.

(Key words: Aftershock, Focal mechanism, JHD, Chiayi)

### 1. INTRODUCTION

On July 17, 1998, a damaging earthquake ( $M_L=6.2$ ) took place in southwestern Taiwan, approximately 25 km to the northeast of Chiayi. The epicenter of the mainshock was located at 23° 30.16' N and 120° 39.75' E with a focal depth of 2.8 km, as estimated by the Central Weather Bureau Seismic Network (CWBSN). The mainshock was felt throughout Taiwan and

---

<sup>1</sup>Institute of Earth Sciences, Academia Sinica, P.O. Box 1-55, Nankang, Taipei, Taiwan, ROC

<sup>2</sup>Central Weather Bureau, Taipei, Taiwan, ROC

<sup>3</sup>Institute of Seismology, National Chung Cheng University, Chiayi, Taiwan, ROC

<sup>4</sup>Institute of Geophysics, National Central University, Chung-Li, Taiwan, ROC

the Penghu islands. It caused landslides, rockfalls and damage to buildings. The rockfalls killed five people and injured more than 25 people. Two days after the occurrence of the mainshock, the Institute of Earth Sciences, Academia Sinica deployed a temporary seismic network (Figure 1) in the epicentral area to monitor the aftershock activity. The network consisted of 15 stations with L4-3D 2 Hz sensors and force-balance accelerometers, and covered an area of 16 km  $\times$  20 km. It was operated for 24 days until 11 August. During the period of operation, 85 events were recorded and located. The deployment of the dense array in the aftershock area was to collect more near-field strong ground motions and to obtain better earthquake locations. In this work, we focus on the study of earthquake locations and focal mechanisms of aftershocks in order to find the correlation between aftershock activity and the faults in the study area. The joint hypocentral determination (JHD) technique (Pujol, 1988) was applied to investigate velocity anomalies and to obtain more reliable earthquake locations by taking care of any lateral velocity anomalies.

## 2. GEOLOGICAL SETTINGS

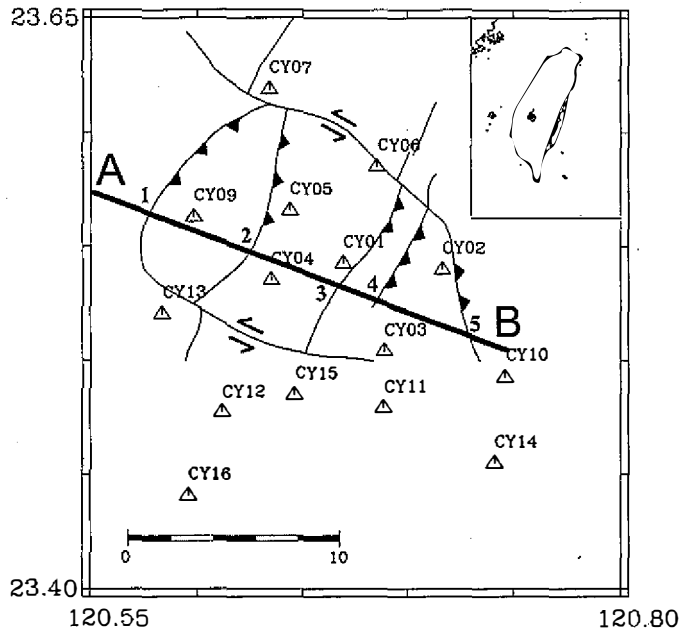
Geologically, the study area is located on the western side of the Western Foothills province. This geologic province consists of a thick sequence of shallow marine to shelf clastic sediments ranging in age from late Oligocene and Miocene to early Pleistocene (Huang, 1980). The rocks in the Western Foothills were deformed by a combination of asymmetric folds and low-angle thrust faults, trending mainly northeast or north and dipping toward the southeast or east with large angles (Ho, 1976; Suppe, 1980). The Chukou fault is one of the major thrusts in this geological province.

The major geological features of the study area are shown in Figure 1. The Tachienshan fault, a segment of the Chukou fault, separates the area into two distinct geologic structures (Liu and Lee, 1998). The structural manifestation to the west of the Tachienshan fault is simple with folds generally more gentle and with fewer faults, while those to the east are complex with tighter folds and many faults (Keng, 1986). The folds striking in the northeast may have been formed during the earlier Penglai Orogeny (Liu and Lee, 1998). The faults trending northeast were probably formed later in the event and were followed by east-west striking and lateral slip faults (Tsan and Keng, 1962; Liu and Lee, 1998).

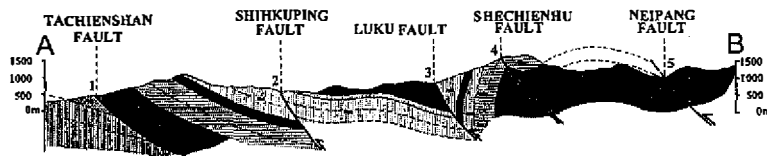
The cross-section inferred from geologic structure is shown in Figure 1b. The major faults in the study area include the Tachienshan fault, the Shihkoping fault, the Luku fault, the Shechiunhu fault and the Neipang fault. Each of these faults is characterized by thrust faulting dipping to the southeast. In particular, the thrust plane of the Tachienshan fault dips at a high angle near the surface but more gently at depth. The Tachienshan fault is believed to be a low-angle thrust and may become a sole fault at depth (Keng, 1986).

## 3. DATA COLLECTION AND PROCESSING

In order to increase the capability of detecting aftershock activity, five stations close to the mainshock area were equipped with Kinematics K2 recorders, three-component force-



(a)



(b)

**Fig. 1.** (a) Major geological structures and locations of the portable stations (triangles) in the Ruey-Li, Chiayi area. (b) Structure section along AB profile shown in Figure 1a (after Liu and Lee, 1998). 1. Tachienshan fault, 2. Shihkuping fault, 3. Luku fault, 4. Shechiunhu fault, 5. Neipang fault.

balance accelerometers and 2-Hz three-component seismometers (Mark L4-3D). Each of the rest ten stations was equipped with a Kinematics Enta recorder and a three-component force-balance accelerometer. Trigger threshold was set to 0.04% of full scale (2g) and the sample rate was 200 samples per second. In addition, each station was equipped with a GPS timing system so that the timing is accurate to 0.5 milliseconds. Table 1 lists station locations and the instruments used.

The digital seismic data recorded were converted into PC-SUDS format (Banfill, 1993a;

1993b) for further data analysis. P- and S-wave arrivals were picked using an efficient phase-picking program, SUDSPK (Chen et al., 1993). During the period of operation from 19 July to 11 August, more than 100 events were recorded by at least two of the 15 stations, and earthquakes which were recorded by more than three stations were selected for location. Earthquake locations were determined using the computer program HYPOELLIPSE (Lahr, 1989). The velocity model (Table 2) inferred by Chen (1995) from P- and S-wave arrival times of local earthquakes beneath southwestern Taiwan was used.

#### 4. AFTERSHOCK ACTIVITY AND ACTIVE FAULTS

According to the CWBSN report, nearly 500 aftershocks took place in the first three days after the mainshock, and then the aftershock activity decreased markedly from hundreds to several events per day. During the period of the aftershock survey, 85 events were recorded and located. Locations of these aftershocks are shown in Figure 2. Obviously, most aftershocks were located in a small area to the north of the mainshock. Two cross-sections of aftershocks along AA' and BB' (see Figure 2a), approximately perpendicular and parallel to the major geological structure in the study area, are shown in Figure 2b. The events were

Table 1. Station locations of the portable seismic network and instruments used in the Chiayi area.

Station Code	Instrument Used	Latitude (deg.-min.-sec.)	Longitude (deg.-min.-sec.)	Elevation (meters)	Period of operation
CY01	K2&SS*	23-32-33.98	120-40-06.09	1060	98/07/19-98/08/11
CY02	ETNA	23-32-22.6	120-42-59.18	838	98/07/19-98/08/11
CY03	ETNA	23-30-14.47	120-41-20.27	1337	98/07/19-98/08/11
CY04	K2&SS*	23-32-06.39	120-38-05.16	1025	98/07/19-98/08/11
CY05	K2&SS*	23-33-56.21	120-38-37.21	715	98/07/19-98/07/24**
CY06	ETNA	23-35-05.74	120-41-07.97	765	98/07/19-98/08/11
CY07	ETNA	23-37-07.74	120-38-02.49	600	98/07/19-98/08/11
CY09	ETNA	23-33-46.38	120-35-52.52	956	98/07/19-98/08/11
CY10	ETNA	23-29-33.96	120-44-47.02	1510	98/07/19-98/07/24**
CY11	K2&SS*	23-28-45.46	120-41-20.27	1395	98/07/19-98/08/11
CY12	ETNA	23-28-36.5	120-36-43.37	713	98/07/19-98/08/11
CY13	ETNA	23-31-12.45	120-35-00.65	227	98/07/19-98/08/11
CY14	ETNA	23-27-17.9	120-44-28.07	960	98/07/19-98/08/11
CY15	K2&SS*	23-29-04.77	120-38-47.36	665	98/07/19-98/08/11
CY16	ETNA	23-26-25.72	120-35-45.32	237	98/07/19-98/08/11
CY17	ETNA	23-33-56.21	120-38-37.21	715	98/07/24-98/08/11**
CY18	K2&SS*	23-29-33.96	120-44-47.02	1510	98/07/24-98/08/11* *

\*K2 digital recorder with additional 3 channels equipped with short-period velocity sensor.

\*\*The locations of CY17 and CY18 are the same as CY05 and CY10, respectively, but we exchanged instruments between these locations on July 24.

Table 2. Velocity model of southwestern Taiwan (Chen, 1995).

Depth (km)	Vp (km/sec)	Vs (km/sec)
0.0	3.49	1.96
2.0	4.30	2.49
4.0	5.05	2.89
9.0	5.70	3.29
13.0	6.00	3.49
17.0	6.31	3.63
25.0	6.80	3.91
30.0	7.30	4.21
35.0	7.79	4.50
50.0	8.18	4.79

located in the upper crust and the focal depths were mainly shallower than 10 km. Most of the aftershocks occurred at depths deeper than the mainshock. The profile (AA') seems to show a southeasterly dipping plane which may be associated with the Luku fault and the Shihkuping fault.

In order to find any correlation between aftershock activity and the known active faults, the collected aftershocks were relocated using a joint hypocentral determination (JHD) technique (Pujol, 1988). This technique has been successfully used to detect lateral velocity variations and to improve relative earthquake locations in various tectonic regions (e.g., Pujol, 1995; Ratchkovsky et al., 1997). The JHD method can simultaneously solve the station corrections and the hypocentral parameters. Positive and negative station corrections correspond to low- and high-velocity anomalies, respectively. The station corrections partially compensate for the lateral velocity variations, and thus can be applied to improve the accuracy of the relative hypocenter locations.

The P- and S-wave station corrections determined from the JHD method are shown in Figure 3. It is obvious that the patterns of station corrections correlate well with the major surface geological features in the study area. Eastern and western parts of the study area are characterized by negative and positive station corrections, respectively. The station corrections vary from 0.30 to -0.18 sec for the P waves and from 0.51 to -0.58 sec for the S waves. The magnitude of P- and S-wave station corrections decreases gradually and then increases from east to west.

Comparison of the JHD hypocenter locations with the initial locations shows a systematic pattern in hypocenter shift. Figure 4 shows epicentral distribution and cross-sectional plots of the hypocenters before and after the JHD relocation. In general, the JHD locations have consistently shifted about 1.1 km to the west, 0.4 km to the north and depths increased by 0.7 km in comparison with those determined using a traditional single-event location method. The epicentral distribution of the relocated aftershocks becomes less scattered (Figure 5a). The depth cross-section of the relocated aftershocks (Figure 5b) shows a pattern of seismicity quite different from that shown in Figure 2b. The aftershock activity is mainly concentrated in the depth range between 3 and 8 km. The relocated aftershocks show the more concentrated pat-

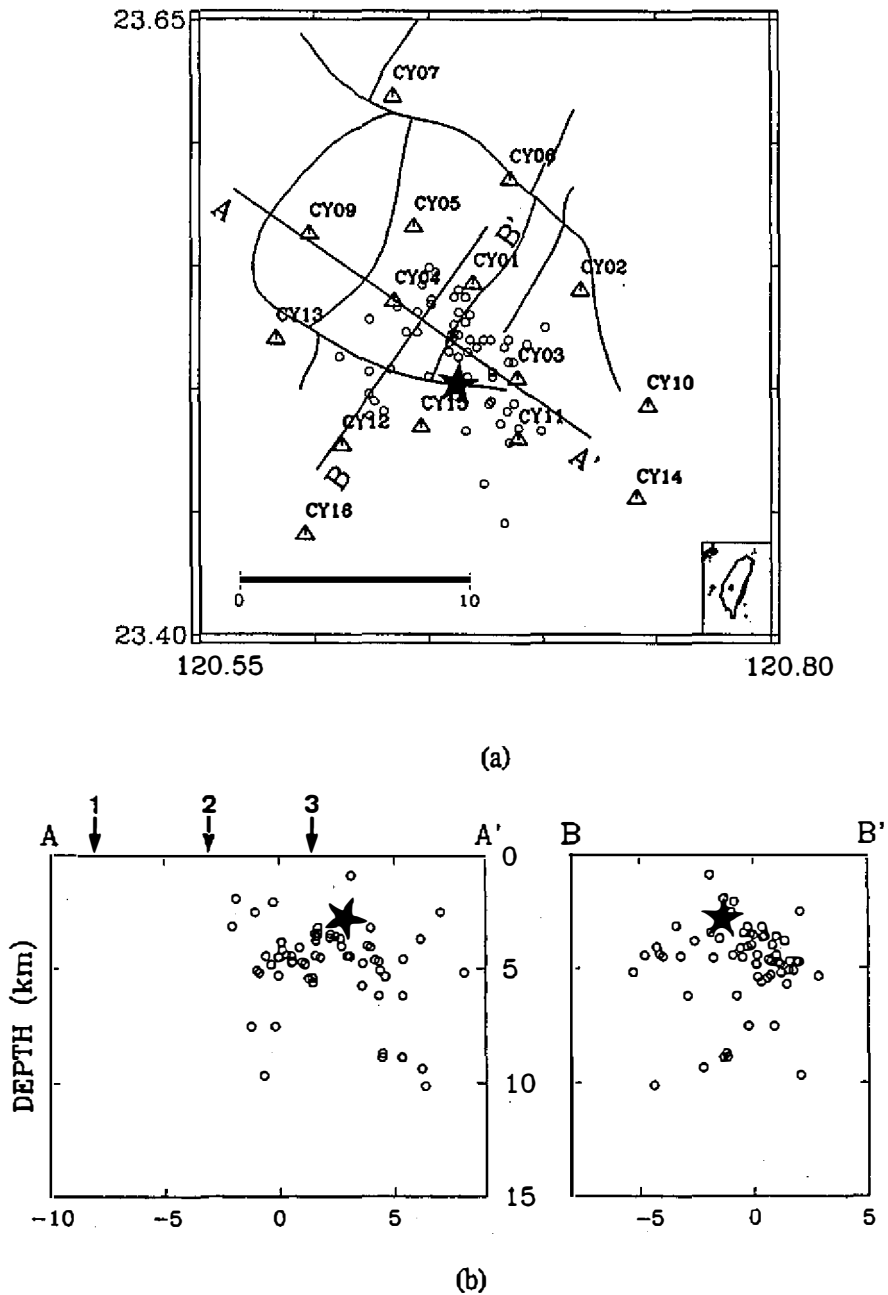
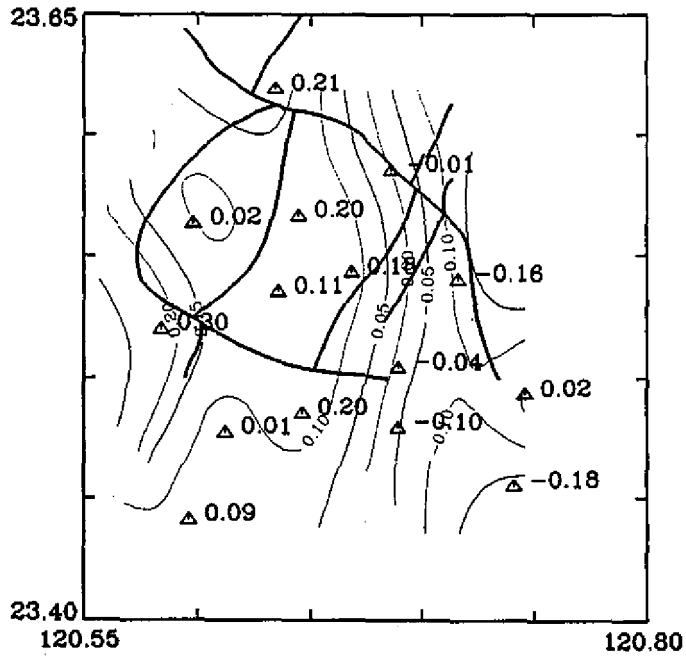
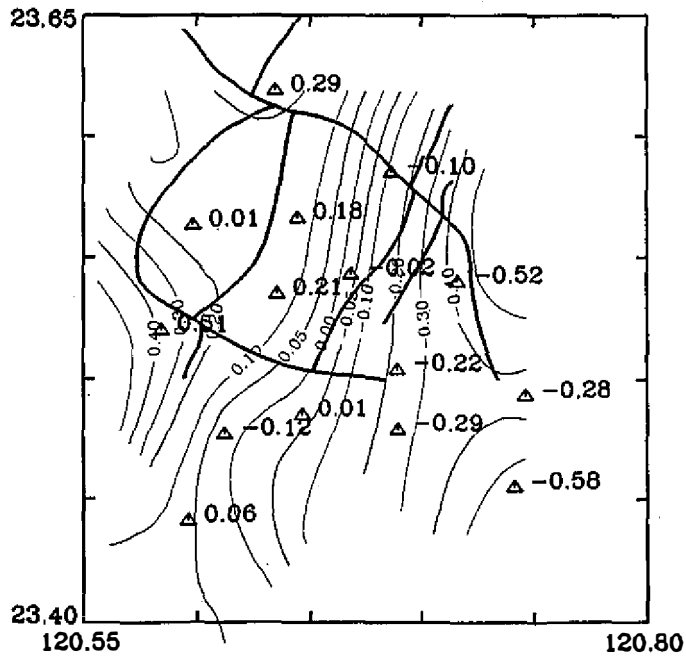


Fig. 2. (a) Epicentral distribution of the aftershocks (circles) recorded by the portable array and station locations (triangles). (b) Depth cross-section of the aftershock hypocenters perpendicular to the major structure shown in Figure 2a. Star denotes location of the mainshock located by CWBSN. Arrows correspond to the fault intersections shown in Figure 1.



(a)



(b)

Fig. 3. Station corrections of (a) P-wave and (b) S-wave in the Ruey-Li, Chiayi area.

tern of a southeast-dipping zone with a dip angle of about  $45^\circ$ . The surface projection of this southeast dipping zone is close to the trace of the Shihkuping fault. Alternatively, this dipping plane can also be associated with the Tachienshan fault, which is a low-angle thrust fault (Keng, 1986).

## 5. FOCAL MECHANISMS

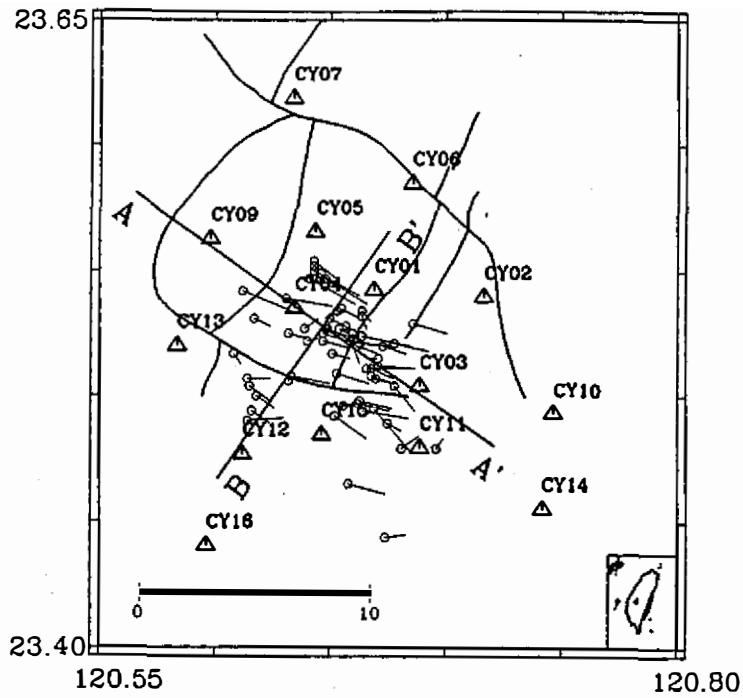
Focal mechanisms of the aftershocks are determined from first-motion polarity data. A grid-search algorithm is used to determine all possible mechanisms fitting with the P-wave polarity data for each earthquake (Snook et al., 1984). Source-station takeoff angles and azimuths are based on the results of JHD relocations. Six well-constrained focal mechanism solutions are derived. The related source parameters are shown in Table 3. The focal depths range from 3.8 km to 7.4 km, and the magnitude values are in the range of 2.4 to 3.3. Figure 6 shows the mechanisms of the six events in map view with the epicenters determined from the JHD relocations. The quality of the mechanisms can be evaluated from Figure 7, which shows the focal mechanism solutions and polarity data.

The focal mechanisms of the aftershocks are predominantly thrust types with southeast compression which is nearly horizontal. They can be characterized into two groups. One group exhibits almost pure thrust dipping to the southeast and northwest. Examination of the distribution of the relocated hypocenters shown in Figure 6 reveals that the northeasterly trending nodal plane ( $N30^\circ\sim35^\circ E$ ) with a dip to the southeast ( $38^\circ\sim46^\circ SE$ ) is spatially consistent with the Tachienshan and Shihkuping faults. The other group displays northerly and northeasterly trending nodal planes with left-lateral and right-lateral motion, respectively. The northeasterly trending nodal plane seems to be consistent with the orientation of the Luku fault. However, this nodal plane dipping to the northwest is contrary to the observation of the Luku fault. Therefore, the northerly trending nodal plane ( $N8^\circ\sim15^\circ W$ ) with a high dip angle to the east ( $71^\circ\sim77^\circ E$ ) is most probably the fault plane.

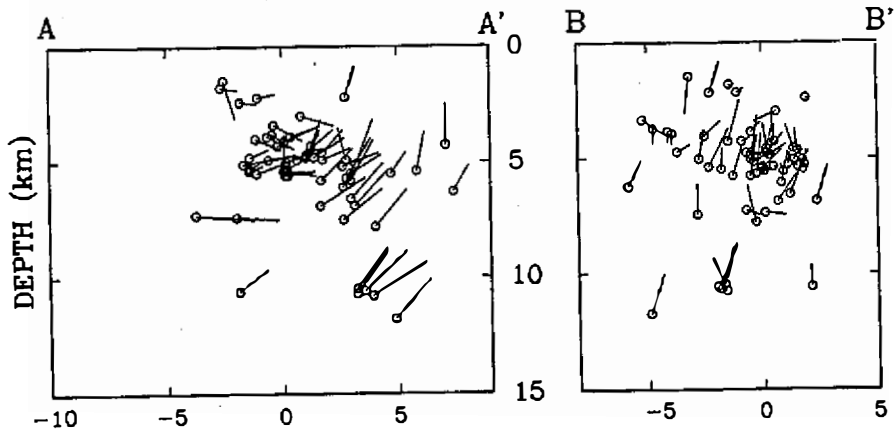
## 6. DISCUSSION

The aftershocks of the Ruyi-Li, Chiayi earthquake recorded by the temporary seismic array were relocated using the JHD method (Pujol, 1988). The large variations of P- and S-wave station corrections estimated from the JHD analysis indicate a significant lateral velocity variation in the study area. The station corrections vary from 0.30 to -0.18 sec for the P waves and from 0.51 to -0.58 sec for the S waves. The stations on the eastern side of the study area are characterized by negative station corrections, while those on the western side are characterized by positive station corrections. A positive station correction indicates that the observed travel time is larger than that calculated from a given velocity model, suggesting that the actual velocity structure is lower than that given by the velocity model used in earthquake location. Similarly, a negative station correction suggests that the actual velocity structure is higher. Therefore, the patterns of station corrections (Figure 3) suggest that the velocities on the eastern side of the study area are relatively higher than those on the western side. The positive



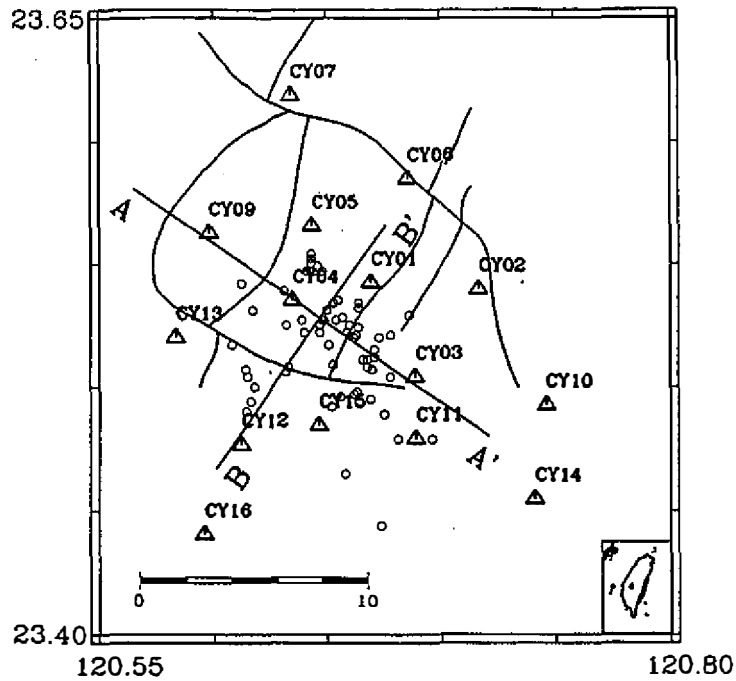


(a)

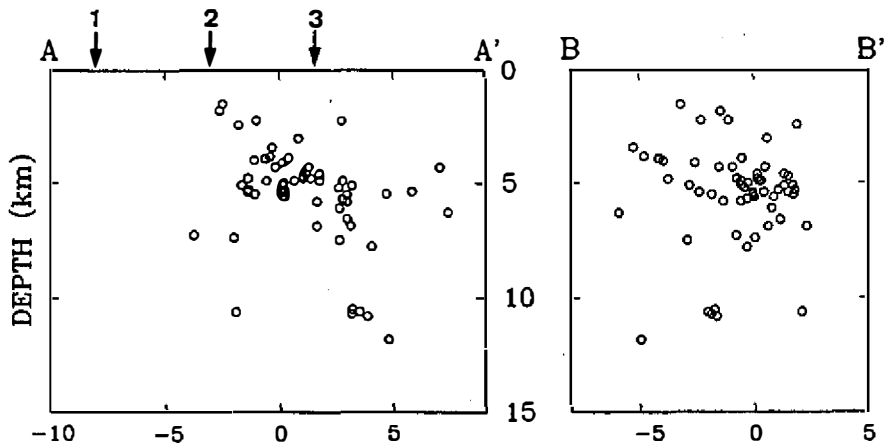


(b)

Fig. 4. (a) Epicentral distribution and (b) cross-sectional plots of the hypocenters, before and after the JHD relocation. The JHD-relocated hypocenter is indicated by a circle and a line is drawn from the initial to the JHD location.



(a)



(b)

Fig. 5. (a) Epicentral distribution of the JHD relocated aftershocks (circles) and station locations (triangles). (b) Depth cross-section of the JHD relocated aftershock hypocenters. Arrows correspond to the fault intersections shown in Figure 1.

Table 3. Source parameters of aftershocks.

No.	Origin Time	Latitude (deg.-min.)	Longitude (deg.-min.)	Depth (km)	Magnitude ( $M_L$ )	Strike (deg.)	Dip (deg.)	Rake (deg.)
01	980722001057.23	23-31.02	120-39.06	4.8	3.3	352.0	71.3	36.0
02	980722222543.30	23-31.62	120-38.88	5.4	3.2	344.4	77.3	38.3
03	980723135336.42	23-32.34	120-37.86	7.4	2.4	30.7	45.9	76.0
04	980727160210.05	23-32.82	120-38.64	5.4	2.8	35.7	37.7	115.0
05	980727162516.55	23-31.62	120-38.94	5.5	3.0	352.0	71.3	36.0
06	980803155108.96	23-29.64	120-36.96	3.8	3.2	35.8	45.9	76.0

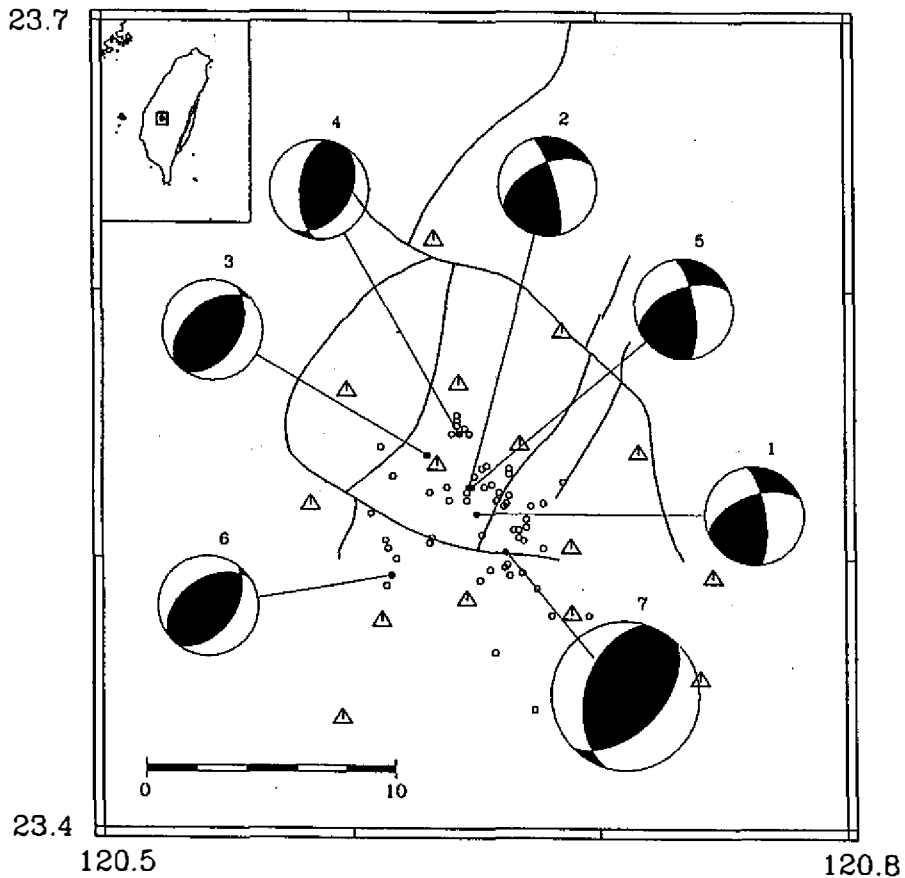


Fig. 6. Aftershock distribution and lower hemisphere focal mechanism solutions for the mainshock (big beach ball, after Chang et al., 1998) and six aftershocks. Compressional quadrants are shaded. The identification numbers refer to Table 3.

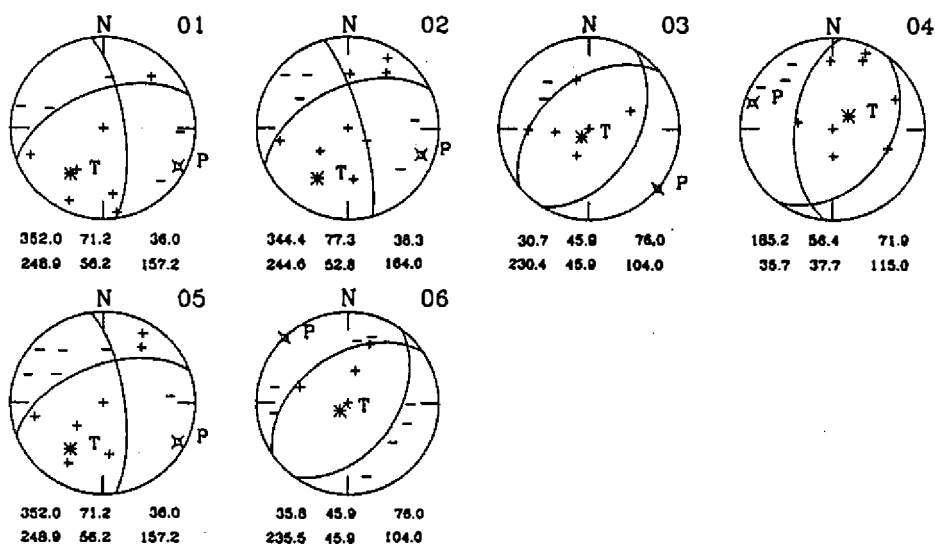


Fig. 7. Lower hemisphere focal mechanism solutions for the Ruey-Li aftershocks. Positive and negative signs indicate compression and dilatation of P-wave polarity, respectively. The label below each mechanism indicates the focal mechanism solutions (strike, dip, and rake) for two nodal planes. The identification number (Table 3) is shown at the upper right corner.

station corrections in the western side of the study area, especially that to the west of the Chukou fault at station CY13, may reflect the presence of thick sediments of lower velocity in the uppermost crust (Liu and Lee, 1998).

The existence of large lateral velocity variations markedly affects the results of earthquake locations determined using the single-event location method. The locations determined using the JHD technique were moved about 1.1 km to the west, 0.4 km to the north and depths increased by 0.7 km in comparison with those determined using a traditional single-event location method. Strong lateral velocity variations may introduce significant errors in the locations of events located individually. The JHD technique, on the other hand, is capable of taking care of lateral variations by first determining station corrections and then applying them to the travel time calculations (Pujol, 1995). The result of a northwestward shift of the JHD locations is consistent with the interpretation of a lower velocity in the upper crust on the western side of the study area.

The JHD relocations of the Ruey-Li aftershocks show the pattern of a southeast-dipping zone. Although the surface projection of this southeast dipping seismic zone is not clear because of its depths from 3 to 8 km, this dipping zone is most probably associated with the Tachienshan and Shihkuping faults. The Tachienshan fault is believed to be a low-angle thrust and may become a sole fault at depth (Keng, 1986), indicating that the Tachienshan and Shihkuping faults might eventually merge together. A focal depth of 6 km for the mainshock,

estimated by Chang *et al.*, (1998) and Wu *et al.*, (1998), put the mainshock location within the southeast-dipping zone. Therefore, the aftershock activity seen in cross-section AA' (Figure 5b) may correspond to the rupture along the same fault plane as that of the mainshock.

The fault-plane solution for the mainshock with a strike of N45°E, a dip of 50°SE, and a rake of 110° (Chang *et al.*, 1998; Wu *et al.*, 1998) is essentially comparable with those of the aftershocks. The southeast-dipping distribution of seismicity and the fault-plane solutions for the aftershocks indicate that the aftershock activity of the Ruey-Li earthquake is most likely associated with the Tachienshan and Shihkukuping faults. The mainshock and six larger-sized aftershocks show thrust faulting. The orientation of P-axes displays southeastward compression, suggesting that thrust faults appearing in the Ruey-Li, Chiayi area may be mainly caused by the northwestern movement of the Philippine Sea plate in relation to the Eurasian plate.

## 7. CONCLUSIONS

Two days after the occurrence of the 17 July 1998 Ruey-Li, Chiayi earthquake, a total of 15 temporary seismic stations was deployed in the epicentral area to monitor aftershock activity. The majority of the Ruey-Li aftershocks took place in the first three days after the mainshock. The aftershock activity dramatically decreased in a very short time period from hundreds to few events per day. Unfortunately, only 85 aftershocks were recorded by the dense portable array during the 24-day deployment. However, the high quality data collected enabled us to extract valuable information about aftershock activity, focal mechanisms and velocity variations in the study area.

The aftershocks of the Ruey-Li earthquake recorded by the temporary seismic stations were relocated using the JHD method (Pujol, 1988). The results show a northwestward shift of 1.2 km for the JHD locations, which is consistent with the interpretation of a lower velocity in the upper crust on the western side of the study area. The JHD relocations of the aftershocks show the pattern of a southeast-dipping zone, which is consistent with the focal mechanisms from the mainshock and aftershocks. Our limited data suggest that the aftershock activity may be associated with the Tachienshan and Shihkukuping faults. Whether the aftershock activity in the first three days took place along our inferred rupture plane remains to be examined. Further study to integrate seismic data recorded by the dense array and recordings of the complete aftershock sequence from CWBSN will definitely be important in resolving this issue.

**Acknowledgements** This study was supported by the Institute of Earth Sciences, Academia Sinica. The Seismological Observation Center of the Central Weather Bureau provided 10 strong motion instruments for data collection. We thank J. Pujol for permission to use the JHD package. We also appreciate the helpful comments on the manuscript made by J.H. Wang, C.Y. Wang, and J.M. Chiu. We thank colleagues at our institute for helping us in the field.

## REFERENCES

Banfill, R., 1993a: PC-SUDS: The Seismic Unified Data System for DOS, Version 1.42,

- Open-file Report, Small Systems Support, UT, 50 pp.
- Banfill, R., 1993b: PC-SUDS utilities: A collection of programs for routine processing of seismic data stored in the Seismic Unified Data System for DOS (PC-SUDS), Open-file Report, Small Systems Support, UT, 91 pp.
- Chang, Z. S., T. C. Shin, and C. Y. Wang, 1998: Ruey-Li earthquake in 1998, Proceedings of the 7<sup>th</sup> Taiwan Symposium on Geophysics, 1-12 (in Chinese).
- Chen, K. C., Y. H. Yeh, Y. T. Yeh, and J. M. Chiu, 1993: The PANDA II system and its softwares for seismic data processing, Open-File Report, Institute of Earth Sciences, Academia Sinica, 28 pp.
- Chen, Y. L., 1995: Three-dimensional velocity structure and kinematic analysis in the Taiwan area, Master's Thesis, National Central University, 172pp (in Chinese).
- Ho, C. S., 1976: Foothills tectonics of Taiwan. *Bull. Geol. Surv. Taiwan*, **25**, 9-28.
- Huang, T. C., 1980: Oligocene to Pleistocene calcareous nannofossil biostratigraphy of the Hsuen Shan Range and western foothills in Taiwan, In: T. Kobayashi et al., (Eds), *Geology and Paleontology of Southeast Asia*, Univ. of Tokyo Press, Tokyo, **21**, 191-210.
- Keng, W.P., 1986: Geology of the area between Chushan and Chiayi, central Taiwan, *Bull. Central Geol. Surv.*, **4**, 1-26 (in Chinese).
- Lahr, J. C., 1989: HYPOELLIPSE/version 2.00: a computer program for determining local earthquake hypocentral parameters, magnitude, and first motion pattern, U.S. Geol. Surv. Open-File Rept. **89-116**.
- Liu, H. C. and J. F. Lee, 1998: Explanatory text of the geologic map of Taiwan: scale 1:50,000, sheet 38, Central Geol. Surv. Open-File Rept. 47pp (in Chinese).
- Ratchkovsky, N. A., Pujol, J., and Biswas N.N., 1997: Relocation of earthquakes in the Cook inlet area, south central Alaska, using the hypocenter determination method. *Bull. Seism. Soc. Am.*, **87**, 620-636.
- Pujol, J., 1988: Comments on the joint determination of hypocenters and station corrections. *Bull. Seis. Soc. Am.*, **78**, 1179-1189.
- Pujol, J., 1995: Application of the JHD technique to the Loma Prieta, California, mainshock-aftershock sequence and implications for earthquake location. *Bull. Seism. Soc. Am.*, **85**, 129-150.
- Snoke, J. A., J. W. Munsey, A. G. Teague, and G. A. Bollinger, 1984: A program for focal mechanism determination by combined use of polarity and SV-P amplitude ratio data. *Earthquake Notes*, **55**, 15.
- Suppe, J., 1980: Imbricate structure of Western Foothills belt, south-central Taiwan. *Petrol. Geol. Taiwan*, **17**, 1-16.
- Tsan, S. F., and W. P. Keng, 1962: The strike-slip faulting and the concurrent or subsequent folding in the Alishan area, Taiwan. *Proc. Geol. Soc. China*, **5**, 119-126.
- Wu, Y. M., Z. S. Chang, and T. C. Shin, 1998: Preliminary analysis of the Ruey-Li, Chiayi earthquake in 1998, Proceedings of the 7<sup>th</sup> Taiwan Symposium on Geophysics, 33-46 (in Chinese).